

Exact tunneling solutions in Minkowski spacetime and a candidate for dark energy

Georgios Pastras¹

*Laboratory for Manufacturing Systems and Automation,
Department of Mechanical Engineering and Aeronautics, University of Patras,
Patras, Greece*

E-mail: georgios.pastras.physics@gmail.com

ABSTRACT: We study exact tunneling solutions in scalar field theory for potential barriers composed of linear or quadratic patches. We analytically continue our solutions to imaginary Euclidean radius in order to study the profile of the scalar field inside the growing bubble. We find that generally there is a non-trivial profile of the scalar field, generating a stress-energy tensor, that depending on the form of the potential, can be a candidate for dark energy.

KEYWORDS: Solitons Monopoles and Instantons, Nonperturbative Effects

ARXIV EPRINT: [1102.4567](https://arxiv.org/abs/1102.4567)

¹When this work was completed, the affiliation of the author was SB ITP LPPC, École Polytechnique Fédérale de Lausanne, Lausanne, Switzerland.

Contents

1	Introduction	2
2	Framework	2
2.1	Two kinds of solutions	3
3	A volcanic potential and the field in the interior of the bubble	4
3.1	The approximation	4
3.2	The instanton solution	4
3.3	Condition for not reaching the true vacuum in Euclidean space	6
3.4	The analytical continuation to Lorentzian spacetime	7
3.5	The stress-energy tensor in the interior of the bubble	8
3.6	The decay rate	9
4	A smooth quadratic potential and the size of the emitted bubble	12
4.1	The approximation	12
4.2	Two classes of bounce solutions	12
4.3	Uniqueness of the solution and the radius of the emitted bubble	14
4.4	The decay rate	15
4.5	The second class of solutions for the smooth quadratic potential	16
5	A triangular potential and a candidate for dark energy	17
5.1	The approximation	17
5.2	The bounce solution	18
5.3	The analytical continuation to Lorentzian spacetime	19
5.4	Asymptotic behavior of the solution	21
5.5	The stress-energy tensor in the interior of the bubble	22
5.6	A candidate for dark energy	23
6	The asymptotic damped oscillation inside the bubble	24
6.1	The asymptotic solution for potential $V = a(\phi - \phi_0)^n$	24
6.2	The stress-energy tensor and the equation of state of the dark matter candidate	26
6.3	Inhomogeneities in the dark content	27
7	Discussion	28

1 Introduction

In quantum field theory containing scalars, it may occur that there are more than one local minima in configuration space. In such cases, a system trapped in a metastable vacuum will decay towards a vacuum with lower energy through quantum tunneling. Semiclassical methods can be used to describe the procedure [1, 2]. In this approach, the theory is studied in Euclidean space and a classical tunneling solution that matches the appropriate boundary conditions is constructed. This solution describes a bubble, which separates the true vacuum from the false vacuum and after its emission starts expanding asymptotically with the speed of light.

Typically, it is very difficult to find analytic solutions for any given potential that contains a metastable vacuum. The original papers [1, 2] focus on a limit, in which the energy difference between the true and false vacua is small. In this limit, the radius of the emitted bubble is large in comparison to its width, thus the name “Thin Wall Approximation” for this approach. This limit allows for analytical expressions of the bubble emission rates. However, such a limit destroys all other potentially interesting features of the solution, especially in the interior of the bubble.

In order to describe potential barriers that are not appropriate for the thin wall approximation, one can either make a numerical computation, or approximate the potential with another one that is exactly solvable. This approach is used in [3], where a triangular and a rectangular potential are analytically solved and the relevant decay rates are calculated. However, if the actual potential is smooth, such potentials are clearly not a very good approximation for the regions of the two vacua and the top of the barrier, so several qualitative features of the solution, related with these regions of the potential barrier, may be lost. For example, the discontinuity of the potential in the rectangular approximation removes all dynamics as the field rolls towards the true vacuum. Smoother, exactly solvable potentials are studied in [4, 5], where the bounce solutions are calculated.

In this paper, we will extend the study of the triangular model and moreover solve some more realistic, still analytically solvable potentials, and try to extract qualitative features of the related physics, and possible cosmological implications. It is going to turn out that the triangular model with parameters of Planck scale can provide an elegant explanation for the order of magnitude of the measured dark energy density in our universe, failing, however, to provide the appropriate equation of state. Other options based on more singular potentials also exist, predicting the correct order of magnitude for the dark energy.

2 Framework

We are going to study exact tunneling solutions in the simple case of a single scalar field and a potential containing a unique false vacuum. We are particularly interested in analytically continuing our solutions to imaginary Euclidean radius in order to study the evolution of the field profile inside the bubble. The Lagrangian describing our system is

$$\mathcal{L} = \frac{1}{2}(\partial_\mu\phi)^2 - V(\phi), \quad (2.1)$$

where the scalar potential $V(\phi)$ contains the true and a unique false vacuum. From now on, we name the positions of the top of the potential barrier and of the true and false vacua as ϕ_T , ϕ_- and ϕ_+ respectively and the relevant values of the potential V_T , V_- and V_+ .

It has been proven that in scalar field theory the spherically symmetric solutions are favoured [6]. Since the interior of the bubble lies in the true vacuum, it corresponds to an energy gain by the emission of the bubble proportional to the volume of the bubble. On the other hand, the bubble wall has to lie at the potential barrier corresponding to an energy loss by the emission of the bubble proportional to the surface of the bubble. Thus, the fact that spherical bubbles are favoured is intuitively expected, as the sphere maximizes the ratio of volume to surface. So, from now on, we assume that the tunneling solution depends only on the Euclidean radius ρ .

Under the assumption that the solution depends only on the Euclidean radius, the Euclidean field equation is reduced to

$$\ddot{\phi} + \frac{3}{\rho}\dot{\phi} = V'(\phi), \tag{2.2}$$

where the dot implies differentiation with respect to ρ and the prime implies differentiation with respect to the field ϕ . The solution has to obey the following boundary conditions

$$\lim_{\rho \rightarrow \infty} \phi(\rho) = \phi_+, \quad \dot{\phi}(0) = 0. \tag{2.3}$$

In the following sections, we are going to make assumptions for the form of the potential, that are going to allow us to find analytic solutions.

2.1 Two kinds of solutions

Before we proceed to solve the equation of motion, we would like to make a comment on the general form of the solutions. Typically we are going to assume that the potential is described by different formulas before and after the top of the barrier. One would expect that we would result in a solution of the form

$$\phi = \begin{cases} \phi_-, & \rho < R_- \\ \phi_1(\rho), & R_- < \rho < R_T \\ \phi_2(\rho), & R_T < \rho < R_+ \\ \phi_+, & \rho > R_+. \end{cases} \tag{2.4}$$

This describes a bubble whose profile can be described as following: outside a certain radius R_+ the field rests in the false vacuum. Inside this radius the field climbs the barrier between R_+ and R_T and then rolls down to the true vacuum between R_T and R_- and then stays there. In such cases the analytic continuation to imaginary Euclidean radius is trivially $\phi = \phi_-$. In [3] we see that in the rectangular approximation, tunneling solutions always look like that, however in the triangular approximation we may get a solution of this kind or not depending on the parameters of the potential. In the triangular approximation, and as we will show later on in other cases, it may be true that the field never reaches the true vacuum in Euclidean space. The conditions leading to such a result in the triangular

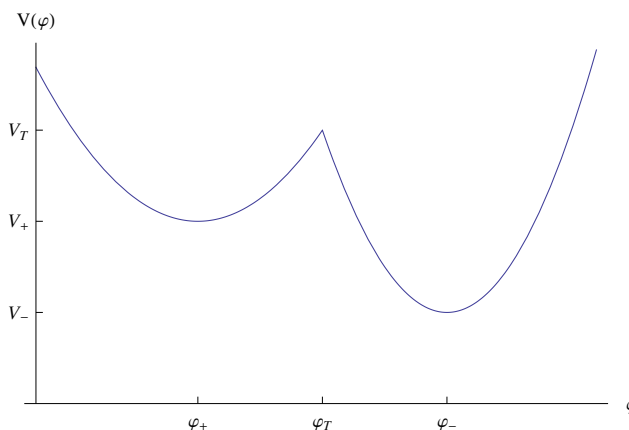


Figure 1. The volcanic approximation.

approximation are not very restricting on the parameters of the potential. In such cases the solution is of the following form

$$\phi = \begin{cases} \phi_1(\rho), & \rho < R_T \\ \phi_2(\rho), & R_T < \rho < R_+ \\ \phi_+, & \rho > R_+ \end{cases} \quad (2.5)$$

and the analytic continuation to imaginary proper time is non trivial. We will show that actually the field in such cases never reaches the true vacuum, but performs a damped oscillation around it. The rest of the paper focuses in this class of solutions.

3 A volcanic potential and the field in the interior of the bubble

3.1 The approximation

The only selections of potential that preserve the linearity of the equation of motion is a linear and a quadratic one. The quadratic is naturally the most obvious selection to approximate the region around a vacuum, thus we will start our analysis studying a potential barrier built out of quadratics. The simplest possible barrier potential built by quadratics is described by

$$V(\phi) = \begin{cases} \frac{1}{2}m_+^2(\phi - \phi_+)^2 + V_+, & \phi < \phi_T \\ \frac{1}{2}m_-^2(\phi - \phi_-)^2 + V_-, & \phi > \phi_T \end{cases} \quad (3.1)$$

and looks like in figure 1. Because of the shape of such a potential, we will call this the volcanic approximation.

3.2 The instanton solution

In order to find the tunneling solution we need to find the general solution to the equation

$$\ddot{\phi} + \frac{3}{\rho}\dot{\phi} = m^2(\phi - \phi_0). \quad (3.2)$$

If we make the substitution

$$\phi - \phi_0 = \frac{y}{\rho}, \tag{3.3}$$

the equation is written as

$$\rho^2 \ddot{y} + \rho \dot{y} - (m^2 \rho^2 + 1)y = 0, \tag{3.4}$$

which is exactly the modified Bessel equation, $x^2 y'' + xy' - (x^2 + \alpha^2)y = 0$ for $x = m\rho$ and $\alpha = 1$. Thus, the general solution is

$$\phi = \phi_0 + \frac{c_1 I_1(m\rho) + c_2 K_1(m\rho)}{\rho}, \tag{3.5}$$

where I_n is the modified Bessel function of the first kind and K_n the modified Bessel function of the second kind. During the construction of the instanton solution, we are going to need the derivative of the solution. This is given by

$$\dot{\phi} = m \frac{c_1 I_2(m\rho) - c_2 K_2(m\rho)}{\rho}. \tag{3.6}$$

Using the above result, it is clear that a solution that does not reach the true vacuum in Euclidean space will look like

$$\phi = \begin{cases} \phi_- + \frac{c_{1-} I_1(m-\rho) + c_{2-} K_1(m-\rho)}{\rho}, & \rho < R_T \\ \phi_+ + \frac{c_{1+} I_1(m+\rho) + c_{2+} K_1(m+\rho)}{\rho}, & R_T < \rho < R_+ \\ \phi_+, & \rho > R_+. \end{cases} \tag{3.7}$$

Let's now apply the boundary and matching conditions to specify the undetermined constants c_{1-} , c_{2-} , c_{1+} , c_{2+} and the radii R_T and R_+ . The solution has to be stationary at the origin. As K_1 diverges at the origin, and I_1 is stationary, we get

$$c_{2-} = 0. \tag{3.8}$$

Demanding continuity of the solution and its derivative at $\rho = R_+$ gives us the following two equations

$$c_{1+} I_1(m_+ R_+) + c_{2+} K_1(m_+ R_+) = 0, \tag{3.9}$$

$$c_{1+} I_2(m_+ R_+) - c_{2+} K_2(m_+ R_+) = 0. \tag{3.10}$$

As both modified Bessel functions of the first and second kind are positive, the only solution to this problem for any finite R_+ is $c_{1+} = c_{2+} = 0$. However, as modified Bessel functions of the second kind decrease exponentially at infinity, we have the option that actually R_+ is infinite and

$$c_{1+} = 0. \tag{3.11}$$

Demanding that $\lim_{\rho \rightarrow R_T^-} \phi(\rho) = \lim_{\rho \rightarrow R_T^+} \phi(\rho) = \phi_T$ gives us

$$c_{1-} = -\frac{\phi_- - \phi_T}{I_1(m_- R_T)} R_T, \tag{3.12}$$

$$c_{2+} = \frac{\phi_T - \phi_+}{K_1(m_+ R_T)} R_T. \tag{3.13}$$

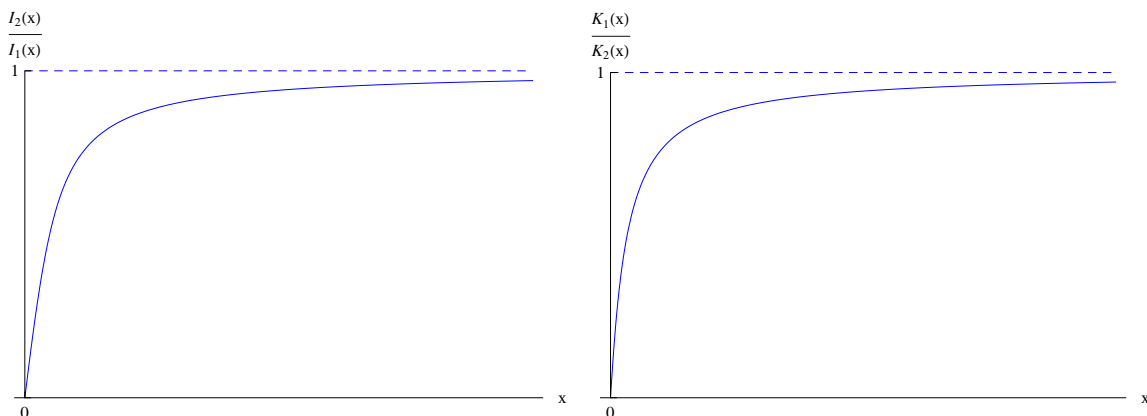


Figure 2. The numerical part of the solution.

We have managed to express all parameters in terms of R_T . Finally demanding continuity of the derivative at $\rho = R_T$, specifies this last unknown parameter. This results in

$$\frac{K_1(m_+R_T) I_2(m_-R_T)}{K_2(m_+R_T) I_1(m_-R_T)} = \frac{m_+ \phi_T - \phi_+}{m_- \phi_- - \phi_T}. \quad (3.14)$$

This equation is not analytically solvable, so we cannot acquire an analytic expression for R_T .

To sum up the tunneling solution is

$$\phi = \begin{cases} \phi_- - \frac{R_T(\phi_- - \phi_T)}{\rho} \frac{I_1(m_- \rho)}{I_1(m_- R_T)}, & \rho < R_T \\ \phi_+ + \frac{R_T(\phi_T - \phi_+)}{\rho} \frac{K_1(m_+ \rho)}{K_1(m_+ R_T)}, & \rho > R_T, \end{cases} \quad (3.15)$$

where R_T is given by (3.14).

3.3 Condition for not reaching the true vacuum in Euclidean space

We expect that in analogy to the triangular approximation [3], if equation (3.14) does not have a solution, the solution reaches the true vacuum in Euclidean space. Functions $\frac{K_1(x)}{K_2(x)}$ and $\frac{I_2(x)}{I_1(x)}$ are both monotonically increasing and take values between zero and one, as one can see in figure 2. Thus there is exactly one bounce solution, as long as

$$\frac{m_+ \phi_T - \phi_+}{m_- \phi_- - \phi_T} < 1, \quad (3.16)$$

otherwise we should expect a bounce solution that reaches the true vacuum in Euclidean space. However, such a solution will look like

$$\phi = \begin{cases} \phi_-, & \rho < R_- \\ \phi_- + \frac{c_{1-} I_1(m_- \rho) + c_{2-} K_1(m_- \rho)}{\rho}, & R_- < \rho < R_T \\ \phi_+ + \frac{c_{1+} I_1(m_+ \rho) + c_{2+} K_1(m_+ \rho)}{\rho}, & R_T < \rho < R_+ \\ \phi_+, & \rho > R_+. \end{cases} \quad (3.17)$$

Demanding continuity and smoothness at $\rho = R_-$, gives us

$$c_{1-} I_1(m_- R_-) + c_{2-} K_1(m_- R_-) = 0, \tag{3.18}$$

$$c_{1-} I_2(m_- R_-) - c_{2-} K_2(m_- R_-) = 0. \tag{3.19}$$

As the modified Bessel function are positive, the only solution to the above system of equations for any $R_- > 0$ is $c_{1-} = c_{2-} = 0$. The only way to save this is to set R_- to zero. Then smoothness at $\rho = R_-$ gives us $c_{2-} = 0$. However then the field has not reached the true vacuum at $\rho = R_-$, as $\lim_{x \rightarrow 0} \frac{I_1(x)}{x} = \frac{1}{2} \neq 0$.

Thus, it looks like finding a solution that reaches the true vacuum in Euclidean space is problematic. Indeed we can see that condition (3.16) is always satisfied. From the expression of the potential (3.1) we can find

$$\frac{m_+ \phi_T - \phi_+}{m_- \phi_- - \phi_T} = \sqrt{\frac{V_T - V_+}{V_T - V_-}}, \tag{3.20}$$

which is always positive and smaller than one since $V_T > V_+ > V_-$

That means that condition (3.16) always holds. Thus, in the volcanic approximation, there is always exactly one tunneling solution, that never reaches the true vacuum in Euclidean space. This implies that we should expect to find some non trivial field profile in the interior of the growing bubble.

3.4 The analytical continuation to Lorentzian spacetime

The solution of the volcanic potential is very easy to analytically continue to imaginary proper time. The modified Bessel functions are analytic functions having the property $I_1(x) = -iJ_1(ix)$, where J_n is the Bessel function of the first kind. Thus, for $\rho = i\tau$ we get

$$\phi(\tau) = \phi_- - \frac{R_T(\phi_- - \phi_T)}{\tau} \frac{J_1(m_- \tau)}{I_1(m_- R_T)}, \tag{3.21}$$

which clearly describes a damped oscillation of the field around the true vacuum in the interior of the bubble. For large τ we can use the asymptotic formula for the Bessel function to get

$$\phi(\tau) \simeq \phi_- + \sqrt{\frac{2}{\pi}} \frac{R_T(\phi_- - \phi_T)}{I_1(m_- R_T)} \frac{\cos(m_- \tau + \frac{\pi}{4})}{\tau^{\frac{3}{2}}}. \tag{3.22}$$

The solution is plotted in figure 3.

In the previous subsection we showed that in the case of the volcanic approximation the field never reaches the true vacuum in Euclidean space. This means that this kind of damped oscillations of the field around the true vacuum in the interior of the bubble, which we discovered by analytically continuing to imaginary Euclidean radius, are present for any parameters of the volcanic potential. As this behaviour is determined by the potential at the region of the true vacuum, the fact that the solution in the case of the triangular or rectangular approximation may be constant for imaginary Euclidean distance [3], is an effect because of the non-smoothness of the potential in the region of the true vacuum. We expect that any smooth potential produces a tunneling solution with the characteristic behaviour of the damped oscillation around the true vacuum in the interior of the bubble.

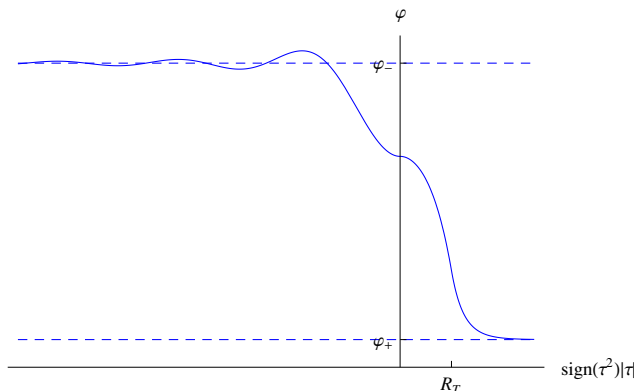


Figure 3. The instanton solution.

3.5 The stress-energy tensor in the interior of the bubble

Under the scope of possible applications in cosmology, it would be interesting to calculate the stress-energy tensor in the interior of the bubble. Unlike traditional treatment, where the stress energy tensor contains only the vacuum energy of the true vacuum, here the damped oscillation around it is going to contribute too.

The stress-energy tensor is given by

$$T^\mu{}_\nu = \frac{\partial \mathcal{L}}{\partial(\partial_\mu \phi)} \partial_\nu \phi - \mathcal{L} \delta^\mu_\nu. \tag{3.23}$$

Substituting our Lagrangian we get

$$T^\mu{}_\nu = \partial^\mu \phi \partial_\nu \phi - \mathcal{L} \delta^\mu_\nu. \tag{3.24}$$

Our solution depends only on proper time, thus

$$\partial_\nu \phi = \dot{\phi}(\tau) \frac{x_\nu}{\sqrt{-x_\mu x^\mu}}. \tag{3.25}$$

Using the above we get

$$T^\mu{}_\nu = \dot{\phi}^2 \frac{x^\mu x_\nu}{x_\lambda x^\lambda} - \mathcal{L} \delta^\mu_\nu. \tag{3.26}$$

The first term of the stress-energy tensor is the kinetic energy of the remnant of the bubble wall inside the bubble. Far away from the bubble wall, it contributes only to the time-time component of the stress-energy tensor, thus it behaves as dark matter. The second term is identical to vacuum energy, that does not only originate from the energy of the true vacuum, but also on the oscillation of the field. We can define

$$\rho_{\text{vac}} = \frac{1}{2}(-\dot{\phi}^2 + m_-^2(\phi - \phi_-)^2) + V_-, \tag{3.27}$$

$$\rho_{\text{wall}} = \dot{\phi}^2. \tag{3.28}$$

Using our solution we get

$$\rho_{\text{vac}} = \frac{m_-^2 R_T^2 (\phi_- - \phi_T)^2}{2I_1(m_- R_T)^2 \tau^2} (-J_1(m_- \tau)^2 + J_2(m_- \tau)^2) + V_-, \quad (3.29)$$

$$\rho_{\text{wall}} = \frac{m_-^2 R_T^2 (\phi_- - \phi_T)^2}{I_1(m_- R_T)^2 \tau^2} J_2(m_- \tau)^2. \quad (3.30)$$

For large τ we can use the asymptotic formula for the Bessel function to get

$$\rho_{\text{vac}} = \frac{m_- R_T^2 (\phi_- - \phi_T)^2}{\pi I_1(m_- R_T)^2 \tau^3} \left[-\sin\left(m_- \tau - \frac{\pi}{4}\right)^2 + \cos\left(m_- \tau - \frac{\pi}{4}\right)^2 \right] + V_-, \quad (3.31)$$

$$\rho_{\text{wall}} = \frac{2m_- R_T^2 (\phi_- - \phi_T)^2}{\pi I_1(m_- R_T)^2 \tau^3} \cos\left(m_- \tau - \frac{\pi}{4}\right)^2. \quad (3.32)$$

As expected from virial theorem, the average of kinetic and potential energy terms in the Lagrangian cancel out, because of the quadratic form of the potential around the true vacuum. However, this kind of ideas can in general provide a cosmological constant that depends on the size of the bubble. It could be a promising candidate for the explanation of the small size of the observed dark energy density.

3.6 The decay rate

The volcanic potential may be used to approximate decay rates of metastable vacua, in the case of a potential that does not fit the requirements for the thin wall approximation. Thus, it is interesting to calculate the decay rate. The decay rate per unit volume is given by

$$\frac{\Gamma}{V} = A e^{-\frac{B}{\hbar}} [1 + \mathcal{O}(\hbar)], \quad (3.33)$$

where coefficient B is given by the Euclidean action of the tunneling solution

$$B = S_E[\phi(\rho)] - S_E[\phi_+]. \quad (3.34)$$

Spherical symmetry of the tunneling solution implies

$$S_E[\phi(\rho)] = 2\pi^2 \int_0^\infty \delta\rho \rho^3 \left(\frac{1}{2} \dot{\phi}(\rho)^2 + V[\phi(\rho)] \right). \quad (3.35)$$

Using the formula of our solution we get

$$\begin{aligned} B = S_E[\phi(\rho)] - S_E[\phi_+] &= 2\pi^2 (V_- - V_+) \int_0^{R_T} \delta\rho \rho^3 \\ &+ \frac{\pi^2 m_-^2 R_T^2 (\phi_- - \phi_T)^2}{I_1(m_- R_T)^2} \int_0^{R_T} \delta\rho \rho [I_1(m_- \rho)^2 + I_2(m_- \rho)^2] \\ &+ \frac{\pi^2 m_+^2 R_T^2 (\phi_T - \phi_+)^2}{K_1(m_+ R_T)^2} \int_{R_T}^\infty \delta\rho \rho [K_1(m_- \rho)^2 + K_2(m_- \rho)^2]. \end{aligned} \quad (3.36)$$

Applying properties of modified Bessel functions, we find

$$\begin{aligned} B &= \frac{\pi^2 (V_- - V_+) R_T^4}{2} \\ &+ \pi^2 m_- R_T^3 (\phi_- - \phi_T)^2 \frac{I_2(m_- R_T)}{I_1(m_- R_T)} + \pi^2 m_+ R_T^3 (\phi_T - \phi_+)^2 \frac{K_2(m_+ R_T)}{K_1(m_+ R_T)}. \end{aligned} \quad (3.37)$$

Finally, using equation (3.14) we find

$$B = \frac{\pi^2(V_- - V_+)R_T^4}{2} + \pi^2 m_+ R_T^3 (\phi_- - \phi_+) (\phi_T - \phi_+) \frac{K_2(m_+ R_T)}{K_1(m_+ R_T)}. \quad (3.38)$$

The first term corresponds to the vacuum energy gained in the volume of the bubble, while the second term corresponds to the energy spent on the bubble wall.

It would be interesting to study whether the decay rate that we just calculated reduces to the known formula in the thin wall limit. In the limit where the energy difference between the true and false vacuum is small, we can derive from the form of the potential that

$$\phi_T = \frac{m_- \phi_- + m_+ \phi_+}{m_- + m_+} + \frac{\varepsilon}{m_- m_+ (\phi_- - \phi_+)} + \mathcal{O}(\varepsilon^2), \quad (3.39)$$

where $\varepsilon \equiv V_+ - V_-$. We can use the above to find

$$\frac{m_+ \phi_T - \phi_+}{m_- \phi_- - \phi_T} = 1 - \frac{\varepsilon}{\mu^2 (\phi_- - \phi_+)^2} + \mathcal{O}(\varepsilon^2). \quad (3.40)$$

That means that the right hand side of equation (3.14) is very close to one, thus R_T has to be large, as expected for the thin wall limit. This allows us to use asymptotic formulas for the modified Bessel functions to approximate the left hand side of (3.14) as

$$\frac{K_1(m_+ R_T)}{K_2(m_+ R_T)} \frac{I_2(m_- R_T)}{I_1(m_- R_T)} = 1 - \frac{3}{2\mu R_T} + \mathcal{O}\left(\frac{1}{R_T^2}\right), \quad (3.41)$$

where

$$\mu \equiv \frac{m_- m_+}{m_- + m_+}. \quad (3.42)$$

So, we can calculate the size of the emitted bubble to be equal to

$$R_T = \frac{3\mu(\phi_- - \phi_+)^2}{2\varepsilon} + \mathcal{O}(\varepsilon^0) \quad (3.43)$$

and finally substituting to formula (3.38) we result in the desired decay rate

$$B = \frac{27\pi^2 \mu^4 (\phi_- - \phi_+)^8}{32\varepsilon^3} + \mathcal{O}\left(\frac{1}{\varepsilon^2}\right). \quad (3.44)$$

In the thin wall approximation, as described in [1], the B factor equals

$$B = \frac{27\pi^2 S_1^4}{2\varepsilon^3}, \quad (3.45)$$

where

$$S_1 = \int_{\phi_+}^{\phi_-} d\phi \sqrt{2V(\phi) - V_-}. \quad (3.46)$$

In our case it is not difficult to calculate S_1 , when the vacua energies are close

$$S_1 = \int_{\phi_+}^{\frac{m_- \phi_- + m_+ \phi_+}{m_- + m_+}} d\phi m_+ (\phi - \phi_+) + \int_{\frac{m_- \phi_- + m_+ \phi_+}{m_- + m_+}}^{\phi_-} d\phi m_- (\phi - \phi) + \mathcal{O}(\varepsilon) \quad (3.47)$$

and after some algebra

$$S_1 = \frac{\mu(\phi_- - \phi_+)^2}{2} + \mathcal{O}(\varepsilon). \quad (3.48)$$

Substituting the latter to (3.45) gives us exactly the same result as (3.44).

Another interesting limit to check is the tunneling without barrier limit, which is discussed in [7]. In our case, this clearly corresponds to the limit $m_+ \rightarrow 0$. In this limit, we can use asymptotic formulas for the modified Bessel functions of the second kind to approximate

$$\frac{K_1(m_+ R_T)}{K_2(m_+ R_T)} = \frac{m_+ R_T}{2} + \mathcal{O}(m_+^2). \quad (3.49)$$

This allows us to write equation (3.14) as

$$\frac{m_- R_T}{2} \frac{I_2(m_- R_T)}{I_1(m_- R_T)} = \frac{\phi_T - \phi_+}{\phi_- - \phi_T}. \quad (3.50)$$

The same asymptotic expansions allow us to write equation (3.38) as

$$B = \frac{\pi^2(V_- - V_+)R_T^4}{2} + 2\pi^2 R_T^2(\phi_- - \phi_+)(\phi_T - \phi_+). \quad (3.51)$$

Now we distinguish two cases. If $\phi_T - \phi_+ \ll \phi_- - \phi_T$ we can use asymptotic expansions of modified Bessel functions for small arguments and equation (3.14) can be written as

$$\frac{(m_- R_T)^2}{8} + \frac{(m_- R_T)^4}{192} + \mathcal{O}(m_-^6 R_T^6) = \frac{\phi_T - \phi_+}{\phi_- - \phi_T}. \quad (3.52)$$

We can solve for R_T

$$R_T^2 = \frac{8}{m_-^2} \frac{\phi_T - \phi_+}{\phi_- - \phi_T} + \frac{8}{3m_-^2} \left(\frac{\phi_T - \phi_+}{\phi_- - \phi_T} \right)^2 + \mathcal{O} \left[\left(\frac{\phi_T - \phi_+}{\phi_- - \phi_T} \right)^3 \right]. \quad (3.53)$$

Substituting in (3.38) and using $V_- - V_+ = \frac{1}{2}m_-^2(\phi_- - \phi_T)^2$ we find

$$B = \frac{16\pi^2(\phi_T - \phi_+)^3(\phi_- - \phi_T)}{3(V_- - V_+)} + \mathcal{O}[(\phi_T - \phi_+)^4]. \quad (3.54)$$

This agrees with the results in [7] up to a factor of 2 that occurs because in our case the rolling region of the potential is quadratic instead of linear.

If $\phi_T - \phi_+ \gg \phi_- - \phi_T$ we can use asymptotic expansions of modified Bessel functions for large arguments and equation (3.14) can be written as

$$\frac{m_- R_T}{2} + \mathcal{O}(m_-^0 R_T^0) = \frac{\phi_T - \phi_+}{\phi_- - \phi_T}. \quad (3.55)$$

Again we solve for R_T

$$R_T^2 = \frac{4}{m_-^2} \left(\frac{\phi_T - \phi_+}{\phi_- - \phi_T} \right)^2 + \mathcal{O} \left[\left(\frac{\phi_T - \phi_+}{\phi_- - \phi_T} \right)^0 \right] \quad (3.56)$$

and substitute in (3.38) to find

$$B = \frac{2\pi^2(\phi_T - \phi_+)^4}{(V_- - V_+)} + \mathcal{O}[(\phi_T - \phi_+)^2], \quad (3.57)$$

which agrees with the results of [7].

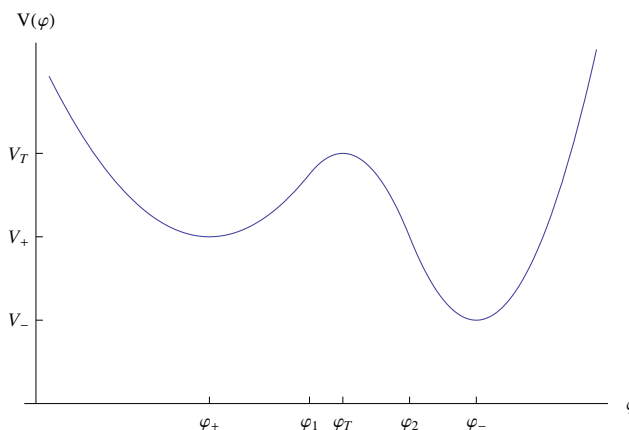


Figure 4. The smooth quadratic approximation.

4 A smooth quadratic potential and the size of the emitted bubble

4.1 The approximation

The volcanic approximation is a bad non-smooth description of the barrier top. We can use the fact that quadratic potentials are solvable, in order to improve our approximation, and search for new qualitative properties of the solutions that originate from the form of the potential at the barrier top. An appropriate approximation is

$$V(\phi) = \begin{cases} \frac{1}{2}m_+^2(\phi - \phi_+)^2 + V_+, & \phi < \phi_1 \\ -\frac{1}{2}m_T^2(\phi - \phi_T)^2 + V_T, & \phi_1 < \phi < \phi_2 \\ \frac{1}{2}m_-^2(\phi - \phi_-)^2 + V_-, & \phi > \phi_2, \end{cases} \quad (4.1)$$

which is plotted in figure 4. Such an approximation provides quite a large flexibility in fitting an arbitrary potential. We can select the above potential in such a way that matches the actual potential in positions and energies of the true and false vacuum, as well as the top of barrier, and moreover the curvature of the potential in these positions or alternatively select it so that it matches the positions and energies of the vacua, as well as one the three aforementioned curvatures and simultaneously be smooth at ϕ_1 and ϕ_2 . The latter case is also studied in [4] in a different context focusing on particle creation at the background off the bounce solution generated by the smooth quadratic potential.

4.2 Two classes of bounce solutions

First we note that at the region between ϕ_1 and ϕ_2 the equation of motion can be solved in exactly the same way as we did in the volcano potential, with the only difference of getting the Bessel functions instead of the modified Bessel function. The equation of motion is

$$\ddot{\phi} + \frac{3}{\rho}\dot{\phi} = m^2(\phi - \phi_0) \quad (4.2)$$

and the general solution can be written as

$$\phi = \phi_0 + \frac{c_1 J_1(m\rho) + c_2 Y_1(m\rho)}{\rho}. \quad (4.3)$$

For later use, we also calculate the derivative of the solution

$$\dot{\phi} = -m \frac{c_1 J_2(m\rho) + c_2 K_2(m\rho)}{\rho}. \quad (4.4)$$

Similarly to the volcanic potential, we expect that there are no solutions that reach the true vacuum in Euclidean space. We separate two classes of bounce solutions in the same way as in [4]. In the first class, the solution does not reach ϕ_2 inside Euclidean space and in the second it does.¹ Here we will study the first class, as it is simpler and it is characterized by interesting qualitative features. Such a solution will look like

$$\phi = \begin{cases} \phi_T + \frac{c_{1T} J_1(m_T \rho) + c_{2T} Y_1(m_T \rho)}{\rho}, & \rho < R_1 \\ \phi_+ + \frac{c_{1+} I_1(m_+ \rho) + c_{2+} K_1(m_+ \rho)}{\rho}, & R_1 < \rho < R_+ \\ \phi_+, & \rho > R_+. \end{cases} \quad (4.5)$$

Exactly as in the volcano potential case, R_+ has to be infinite, and the boundary conditions for the solution imply

$$c_{2T} = 0, \quad (4.6)$$

$$c_{1+} = 0. \quad (4.7)$$

Demanding that $\lim_{\rho \rightarrow R_1^-} \phi(\rho) = \lim_{\rho \rightarrow R_1^+} \phi(\rho) = \phi_1$ gives us

$$c_{1T} = \frac{\phi_1 - \phi_T}{J_1(m_T R_1)} R_1, \quad (4.8)$$

$$c_{2+} = \frac{\phi_1 - \phi_+}{K_1(m_+ R_1)} R_1. \quad (4.9)$$

Finally, smoothness at $\rho = R_1$ implies

$$\frac{K_1(m_+ R_1) J_2(m_T R_1)}{K_2(m_+ R_1) J_1(m_T R_1)} = -\frac{m_+ \phi_1 - \phi_+}{m_T \phi_T - \phi_1}. \quad (4.10)$$

Thus, the instanton solution is given by

$$\phi = \begin{cases} \phi_T - \frac{R_1(\phi_T - \phi_1)}{\rho} \frac{J_1(m_T \rho)}{J_1(m_T R_1)}, & \rho < R_1 \\ \phi_+ + \frac{R_1(\phi_1 - \phi_+)}{\rho} \frac{K_1(m_+ \rho)}{K_1(m_+ R_1)}, & \rho > R_1, \end{cases} \quad (4.11)$$

where R_1 is given by (4.10). Our result agrees with the results of [4].

¹In [4], the first class is described as a bounce solution where the bubble wall does not lie entirely in Euclidean space, while the second class of solutions is described as bounce solutions where the entire bubble wall lies in Euclidean space. In this terminology, the bubble wall is considered to be the region of the bubble where the scalar field takes values in the region where the scalar potential has negative curvature.

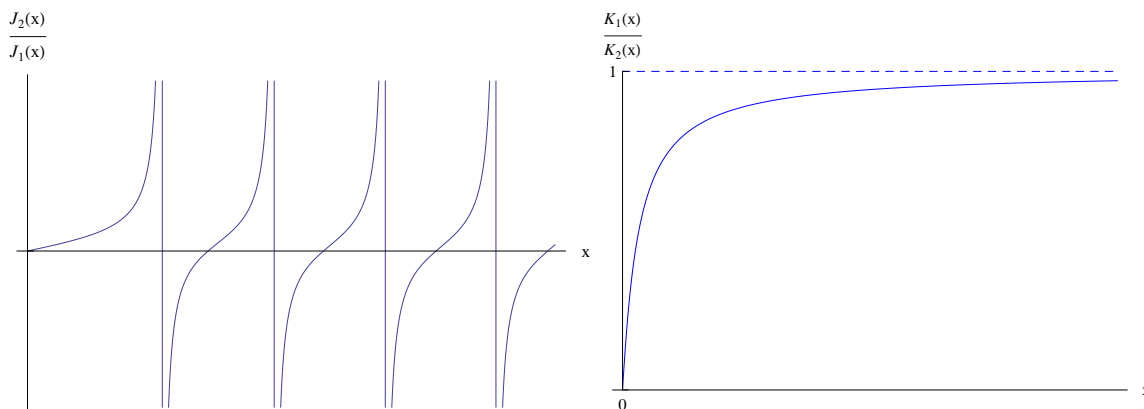


Figure 5. The numerical part of the solution.

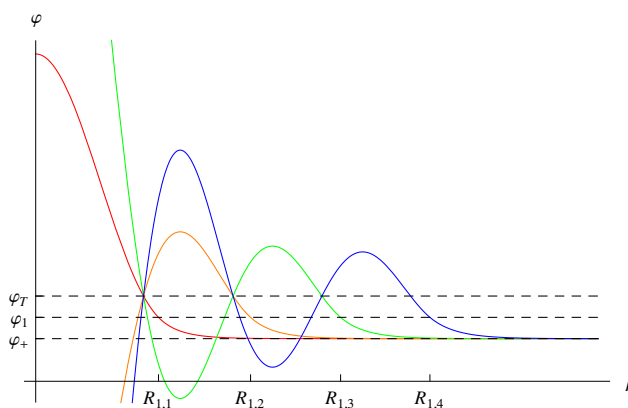


Figure 6. The first solutions in the smooth quadratic approximation.

4.3 Uniqueness of the solution and the radius of the emitted bubble

As in previous cases, the existence or non-existence of a solution is decided by the last equation, that occurs by the demand of smoothness of the solution, in our case equation (4.10). In figure 5, we plot $\frac{K_1(x)}{K_2(x)}$ and $\frac{J_2(x)}{J_1(x)}$. The first graph suggests that we are going to have infinite solutions.

In figure 6, we plot the first solutions. Actually, any other solution except for the first one is not valid, since for all other solutions it is true that in some region of ρ with $\rho < R_1$ region, it holds that $\phi < \phi_1$, on the contrary to what equation (4.11) requires. Let's sketch a proof for that.

The function $\frac{J_1(m_T \rho)}{\rho}$ describes an oscillation whose amplitude decreases monotonically, as it can be seen in figure 6. Based on that and using properties of Bessel functions, one can show that if ρ_S is a stationary point of this function, then

$$\left| \frac{J_1(m_T \rho_S)}{\rho_S} \right| > \frac{J_1(m_T \rho)}{\rho}, \tag{4.12}$$

for any $\rho > \rho_S$. Applying this for $\rho = R_1$ in equation (4.11) it is easy to find that for any

stationary point ρ_S , with $\rho_S < R_1$ it is true that

$$|\phi_S - \phi_T| > \phi_T - \phi_1. \quad (4.13)$$

For any solution except for the first one, there are at least two stationary points in the region $\rho < R_1$, including the one at the origin of the Euclidean space. Because of the oscillatory nature of the solution, for at least one of them, ϕ_S is going to be smaller than ϕ_T . For this point, the above inequality is written as

$$\phi_S < \phi_1. \quad (4.14)$$

For $\phi_S < \phi_1$, the oscillatory solution in terms of Bessel functions is not valid any more, but a solution in terms of modified Bessel functions is required, thus our solution is not valid. This means that any solution except for the first one is not valid and the solution is unique.

This is not a general proof of the uniqueness of the solution for a general potential, however, in this case the oscillatory behaviour of the solution in the region of the barrier top resembles exactly the general behaviour that could produce multiple solutions in general.

So, the only solution it may hold is the first solution, which is valid if $\phi(0) < \phi_2$, or else

$$\frac{2J_1(m_T R_1)}{m_T R_1} < -\frac{\phi_T - \phi_1}{\phi_2 - \phi_T}. \quad (4.15)$$

If this condition does not hold, we should search for a solution of the second class.

Figure 5 implies that the curvature of the potential at the top is strongly related with the size of the emitted bubble. As we stated above, the only valid solution is the one corresponding to the smallest solution of equation (4.10). From figure 5, we can see that this solution always satisfies

$$\frac{\rho_{1,1}}{m_T} < R_1 < \frac{\rho_{2,1}}{m_T}, \quad (4.16)$$

where $\rho_{\alpha,n}$ is the n'th root of J_α . We note that $\rho_{1,1} \simeq 3.83$ and $\rho_{2,1} \simeq 5.14$. This result is identical to the findings of [4].

So the characteristic radius of the emitted bubble is always of the order $\frac{1}{m_T}$. As this class of solutions is the one that actually lies as far as possible from the thin wall approximation, in which the radius of the bubble tends to infinity, we expect that actually $\frac{\rho_{1,1}}{m_T}$ serves as a general lower bound for the radius of the emitted bubble.

4.4 The decay rate

As we did in the volcanic approximation, we can calculate the B factor of decay rate from the Euclidean action. Using the form of our solution we find

$$\begin{aligned} B = S_E[\phi(\rho)] - S_E[\phi_+] &= 2\pi^2(V_T - V_+) \int_0^{R_T} \delta\rho\rho^3 \\ &+ \frac{\pi^2 m_T^2 R_1^2 (\phi_T - \phi_1)^2}{J_1(m_T R_1)^2} \int_0^{R_1} \delta\rho\rho [-J_1(m_T \rho)^2 + J_2(m_T \rho)^2] \\ &+ \frac{\pi^2 m_+^2 R_1^2 (\phi_1 - \phi_+)^2}{K_1(m_+ R_1)^2} \int_{R_1}^\infty \delta\rho\rho [K_1(m_- \rho)^2 + K_2(m_- \rho)^2]. \end{aligned} \quad (4.17)$$

Applying properties of Bessel functions and modified Bessel functions we find

$$B = \frac{\pi^2(V_T - V_+)R_1^4}{2} - \pi^2 m_T R_1^3 (\phi_T - \phi_1)^2 \frac{J_2(m_T R_1)}{J_1(m_T R_1)} + \pi^2 m_+ R_1^3 (\phi_1 - \phi_+)^2 \frac{K_2(m_+ R_1)}{K_1(m_+ R_1)}. \quad (4.18)$$

Finally using equation (4.10) we find

$$B = \frac{\pi^2(V_T - V_+)R_1^4}{2} + \pi^2 m_+ R_1^3 (\phi_T - \phi_+) (\phi_1 - \phi_+) \frac{K_2(m_+ R_1)}{K_1(m_+ R_1)}. \quad (4.19)$$

As in the volcanic potential, the first term corresponds to the vacuum energy gained in the volume of the bubble, while the second term corresponds to the energy spent on the bubble wall.

4.5 The second class of solutions for the smooth quadratic potential

An instanton belonging in the second class will be of the form

$$\phi = \begin{cases} \phi_- + \frac{c_{1-} I_1(m_- \rho)}{\rho}, & \rho < R_2 \\ \phi_T + \frac{c_{1T} J_1(m_T \rho) + c_{2T} Y_1(m_T \rho)}{\rho}, & R_2 < \rho < R_1 \\ \phi_+ + \frac{c_{2+} K_1(m_+ \rho)}{\rho}, & \rho > R_1, \end{cases} \quad (4.20)$$

where we have already embodied the necessary boundary conditions. Demanding that $\phi(R_1) = \phi_1$ and $\phi(R_2) = \phi_2$ and continuity results in

$$c_{1-} = \frac{\phi_2 - \phi_-}{I_1(m_- R_2)} R_2, \quad (4.21)$$

$$c_{2+} = \frac{\phi_1 - \phi_+}{K_1(m_+ R_1)} R_1 \quad (4.22)$$

and

$$c_{1T} = -\frac{Y_1(m_T R_2)(\phi_T - \phi_1)R_1 - Y_1(m_T R_1)(\phi_2 - \phi_T)R_2}{J_1(m_T R_1)Y_1(m_T R_2) - J_1(m_T R_2)Y_1(m_T R_1)}, \quad (4.23)$$

$$c_{2T} = -\frac{J_1(m_T R_1)(\phi_2 - \phi_T)R_2 - J_1(m_T R_2)(\phi_T - \phi_1)R_1}{J_1(m_T R_1)Y_1(m_T R_2) - J_1(m_T R_2)Y_1(m_T R_1)}. \quad (4.24)$$

Finally demanding smoothness results in the following set of equations

$$m_T [c_{1T} J_2(m_T R_1) + c_{2T} Y_2(m_T R_1)] = -m_- c_{1-} I_2(m_- R_2), \quad (4.25)$$

$$m_T [c_{1T} J_2(m_T R_2) + c_{2T} Y_2(m_T R_2)] = m_+ c_{2+} K_2(m_+ R_1). \quad (4.26)$$

These two equations provide a solution for R_1 and R_2 . Unfortunately the problem is very complicated, and has to be numerically solved. In figure 7, we show how a solution to this problem looks like.

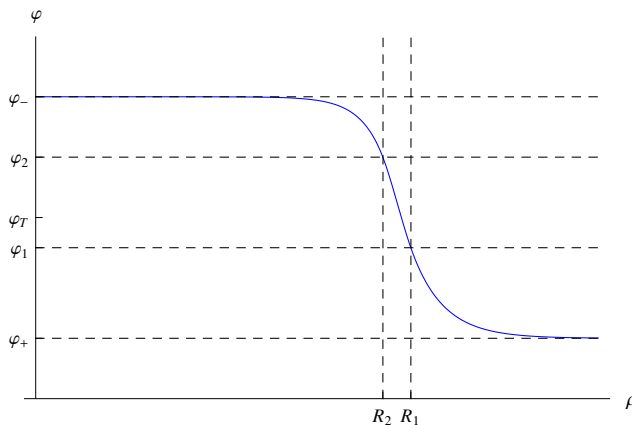


Figure 7. The solution for the smooth quadratic potential.

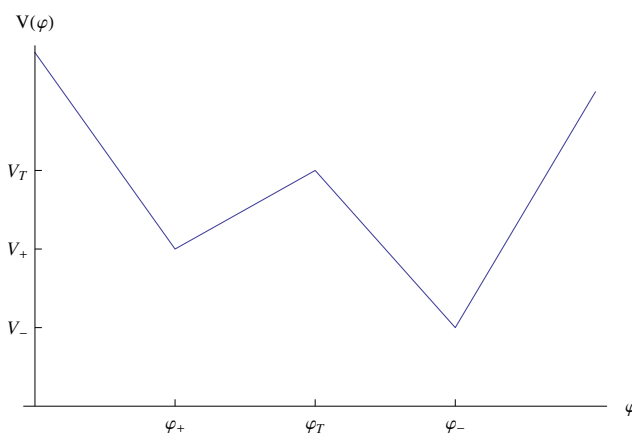


Figure 8. The triangular approximation.

5 A triangular potential and a candidate for dark energy

5.1 The approximation

We will now study the case of a potential barrier approximated by segments of linear potentials. Such a potential looks like in figure 8. This approximation has been analysed in [3]. We review this derivation and then analytically continue to negative proper time.

In the following we use the definitions

$$\Delta V_{\pm} \equiv V_T - V_{\pm}, \quad \Delta \phi_{\pm} \equiv \pm(\phi_T - \phi_{\pm}), \quad (5.1)$$

$$\lambda_{\pm} \equiv \frac{\Delta V_{\pm}}{\Delta \phi_{\pm}}, \quad c \equiv \frac{\lambda_-}{\lambda_+}. \quad (5.2)$$

Using the above definitions, the potential barrier is described by

$$V(\phi) = \begin{cases} \lambda_+(\phi - \phi_+) + V_+, & \phi_+ < \phi < \phi_T \\ -\lambda_-(\phi - \phi_-) + V_-, & \phi_T < \phi < \phi_- \end{cases} \quad (5.3)$$

5.2 The bounce solution

In order to find the appropriate solution we need to solve the equation

$$\ddot{\phi} + \frac{3}{\rho}\dot{\phi} = \lambda. \tag{5.4}$$

It is not difficult to show that the general solution is

$$\phi = \frac{\lambda}{8}\rho^2 + \frac{c}{\rho^2} + K. \tag{5.5}$$

Using the above, an instanton that does not reach the true vacuum in Euclidean space will look like

$$\phi = \begin{cases} -\frac{\lambda_-}{8}\rho^2 + \frac{c_-}{\rho^2} + K_-, & \rho < R_T \\ \frac{\lambda_+}{8}\rho^2 + \frac{c_+}{\rho^2} + K_+, & R_T < \rho < R_+ \\ \phi_+, & \rho > R_+. \end{cases} \tag{5.6}$$

Let's now apply the appropriate boundary and matching conditions to determine the constants c_- , c_+ , K_- , K_+ , as well as the radii R_T and R_+ . The field must be stationary at the origin. This implies that

$$c_- = 0. \tag{5.7}$$

Demanding continuity of the derivative of the field at $R = R_+$ gives us

$$c_+ = \frac{\lambda_+}{8}R_+^4. \tag{5.8}$$

Then we demand continuity at $R = R_+$ and $R = R_T$ and we find

$$K_+ = \phi_+ - \frac{\lambda_+}{4}R_+^2, \tag{5.9}$$

$$K_- = \phi_+ + \frac{\lambda_+}{8R_T^2}(R_+^2 - R_T^2)^2 + \frac{\lambda_-}{8}R_T^2 = \phi_T + \frac{\lambda_-}{8}R_T^2 \equiv \phi_0. \tag{5.10}$$

Continuity of the derivative at $R = R_T$ gives us

$$R_+^4 = (1 + c)R_T^4. \tag{5.11}$$

So far we have expressed all unknowns in terms of the unknown radius R_T . In order to determine this final unknown parameter, we demand that $\phi(R_T) = \phi_T$. We result in

$$\phi_T - \phi_+ = \frac{\lambda_+}{8}(\sqrt{1 + c} - 1)^2 R_T^2. \tag{5.12}$$

Now we have completely determined the tunneling solution. To sum up

$$\phi = \begin{cases} \phi_0 - \frac{\lambda_-}{8}\rho^2, & \rho < R_T \\ \phi_+ + \frac{\lambda_+}{8}\frac{1}{\rho^2}(\rho^2 - R_+^2)^2, & R_T < \rho < R_+ \\ \phi_+, & \rho > R_+, \end{cases} \tag{5.13}$$

where the two radii are given by (5.11) and (5.12) and the value of the field at the origin ϕ_0 is given by (5.10).

If we want our solution to make sense it has to be that $\phi_0 < \phi_-$. Otherwise the field has already reached the true vacuum in Euclidean space. The above condition implies that

$$\frac{\phi_- - \phi_T}{\phi_T - \phi_+} > \frac{c}{(\sqrt{1+c}-1)^2}. \tag{5.14}$$

If this condition holds, the field never reaches the true vacuum in Euclidean space and thus, we expect to perform a damped oscillation around the true vacuum in the interior of the bubble. Otherwise, the field equals exactly to ϕ_- inside a sphere of finite radius in Euclidean space, thus, the analytical continuation for imaginary Euclidean time is trivially $\phi = \phi_-$. Such a solution is well analyzed in [3] and we will not study it here.

5.3 The analytical continuation to Lorentzian spacetime

We are interested in studying the solution for imaginary Euclidean radius. As we commented in section 2.1, this is interesting only if condition (5.14) holds. In such case the solution is given by (5.13). We substitute $\rho = i\tau$ in the formula for the solution that is valid for $\rho < R_T$ to get

$$\phi_0 + \frac{\lambda_-}{8}\tau^2. \tag{5.15}$$

This grows indefinitely as τ decreases. This means that at some finite τ it reaches the true vacuum. After that point, the solution we have is not valid anymore and we need to find an appropriate solution for $\phi > \phi_-$. We approximate the potential around the true vacuum as

$$V(\phi) = \begin{cases} -\lambda^-(\phi - \phi_-) + V_-, & \phi < \phi_- \\ \lambda^+(\phi - \phi_-) + V_-, & \phi > \phi_-, \end{cases} \tag{5.16}$$

where obviously $\lambda^- = \lambda_-$. So, after the τ where the solution reaches the true vacuum, we have to fit a solution of the form

$$\phi = -\frac{\lambda^+}{8}\tau^2 + \frac{c}{\tau^2} + K. \tag{5.17}$$

However this solution will reach a maximum and return to the true vacuum, with some non-vanishing derivative, thus enforcing us to fit again a solution of the form

$$\phi = \frac{\lambda^-}{8}\tau^2 + \frac{c}{\tau^2} + K, \tag{5.18}$$

and so on. So we are going to get an infinite sequence of segments describing a damped oscillation around the true vacuum. So, we need to solve the general problem of fitting a solution of the form (5.17) or (5.18) to the boundary conditions

$$\phi(T_0) = \phi_-, \quad \dot{\phi}(T_0) = \dot{\Phi}_0, \tag{5.19}$$

or else solve the matching conditions

$$\phi_- = \pm \frac{\lambda^\mp}{8} T_0^2 + \frac{c}{T_0^2} + K, \quad (5.20)$$

$$\dot{\Phi}_0 = \pm \frac{\lambda^\mp}{4} T_0 - \frac{2c}{T_0^3}. \quad (5.21)$$

It is not difficult to find that the solution is

$$c = \pm \frac{\lambda^\mp}{8} T_0^4 - \frac{\dot{\Phi}_0 T_0^3}{2}, \quad (5.22)$$

$$K = \phi_- \mp \frac{\lambda^\mp}{4} T_0^2 + \frac{\dot{\Phi}_0 T_0}{2}. \quad (5.23)$$

Once we find the right expression, we need to find the new point where the solution reaches the true vacuum. Demanding that $\phi(T_1) = \phi_-$, we take

$$T_1^2 = T_0^2 \mp \frac{4\dot{\Phi}_0 T_0}{\lambda^\mp}, \quad (5.24)$$

$$\dot{\phi}(T_1) \equiv \dot{\Phi}_1 = -\dot{\Phi}_0 \frac{T_0}{T_1}. \quad (5.25)$$

Thus, we can express the solution inductively as

$$\phi = \begin{cases} -\frac{\lambda^+}{8} \tau^2 + \frac{c_{2n+1}}{\tau^2} + K_{2n+1}, & T_{2n+1} < \tau < T_{2n} \\ \frac{\lambda^-}{8} \tau^2 + \frac{c_{2n}}{\tau^2} + K_{2n}, & T_{2n} < \tau < T_{2n-1}, \end{cases} \quad (5.26)$$

where the constants in solution are given by

$$c_{2n+1} = -\frac{\lambda^+}{8} T_{2n}^4 - \frac{\dot{\Phi}_{2n} T_{2n}^3}{2}, \quad c_{2n} = \frac{\lambda^-}{8} T_{2n-1}^4 - \frac{\dot{\Phi}_{2n-1} T_{2n-1}^3}{2}, \quad (5.27)$$

$$K_{2n+1} = \phi_- + \frac{\lambda^+}{4} T_{2n}^2 + \frac{\dot{\Phi}_{2n} T_{2n}}{2}, \quad K_{2n} = \phi_- - \frac{\lambda^-}{4} T_{2n-1}^2 + \frac{\dot{\Phi}_{2n-1} T_{2n-1}}{2}, \quad (5.28)$$

and the T_n 's and $\dot{\Phi}_n$'s can be calculated inductively by

$$T_{2n}^2 = T_{2n-1}^2 + \frac{4\dot{\Phi}_{2n-1} T_{2n-1}}{\lambda^+}, \quad T_{2n+1}^2 = T_{2n}^2 - \frac{4\dot{\Phi}_{2n} T_{2n}}{\lambda^-}, \quad (5.29)$$

$$\dot{\Phi}_{2n} = -\dot{\Phi}_{2n-1} \frac{T_{2n-1}}{T_{2n}}, \quad \dot{\Phi}_{2n+1} = -\dot{\Phi}_{2n} \frac{T_{2n}}{T_{2n+1}}. \quad (5.30)$$

Finally, the initial values for T and $\dot{\Phi}$ can be easily calculated by equation (5.15), which also defines c_0 and K_0 ,

$$T_0^2 = \frac{8}{\lambda^-} (\phi_- - \phi_0) \quad (5.31)$$

$$\dot{\Phi}_0 = \frac{\lambda^-}{4} T_0. \quad (5.32)$$

The solution is plotted in figure 9.

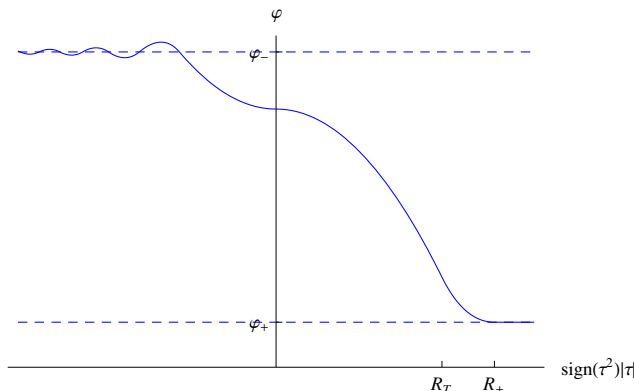


Figure 9. The bounce solution.

5.4 Asymptotic behavior of the solution

For large τ , expressions (5.29) and (5.30) can be approximated by

$$T_{2n+1} \simeq T_{2n} - \frac{2\dot{\Phi}_{2n}}{\lambda^-}, \quad T_{2n} \simeq T_{2n-1} + \frac{2\dot{\Phi}_{2n-1}}{\lambda^+}, \quad (5.33)$$

$$\dot{\Phi}_{2n+1} \simeq -\dot{\Phi}_{2n} \left(1 + \frac{2\dot{\Phi}_{2n}}{\lambda^- T_{2n}} \right), \quad \dot{\Phi}_{2n} \simeq -\dot{\Phi}_{2n-1} \left(1 - \frac{2\dot{\Phi}_{2n-1}}{\lambda^+ T_{2n-1}} \right). \quad (5.34)$$

In order to avoid the alternation of signs in $\dot{\Phi}$, we find recursive relations with step two

$$T_{2n+2} \simeq T_{2n} - 2c\dot{\Phi}_{2n}, \quad (5.35)$$

$$\dot{\Phi}_{2n+2} \simeq \dot{\Phi}_{2n} + 2c\frac{\dot{\Phi}_{2n}^2}{T_{2n}}, \quad (5.36)$$

where $c = \frac{1}{\lambda^-} + \frac{1}{\lambda^+}$. We are interested in finding the asymptotic behavior of T_{2n} and $\dot{\Phi}_{2n}$. We try a solution of the form

$$T_{2n} \simeq an^s, \quad (5.37)$$

$$\dot{\Phi}_{2n} \simeq bn^t. \quad (5.38)$$

The recursive relations at leading order become

$$asn^{s-1} = -2cbn^t, \quad (5.39)$$

$$btn^{t-1} = \frac{2cb^2n^{2t-s}}{a}, \quad (5.40)$$

which imply that

$$s - t = 1, \quad (5.41)$$

$$-as = 2cb, \quad (5.42)$$

$$at = 2cb. \quad (5.43)$$

The solution is

$$s = -t = \frac{1}{2}, \tag{5.44}$$

$$a = -4cb. \tag{5.45}$$

b is undetermined and depends on the initial values for the series, or else in the parameters of the potential. Thus, the asymptotic behaviour of the bounce solution is

$$T_{2n} = -4cb\sqrt{n}, \tag{5.46}$$

$$\dot{\Phi}_{2n} = \frac{b}{\sqrt{n}}. \tag{5.47}$$

Using the above equations, we can find asymptotic expressions for any element of the solution. Combining them, we get

$$\dot{\Phi}_{2n} = -\frac{4cb^2}{T_{2n}}. \tag{5.48}$$

5.5 The stress-energy tensor in the interior of the bubble

Now we know the asymptotic form of the solution, thus we can calculate the asymptotic form of the stress-energy tensor in the interior of the bubble. Equation (5.48) implies

$$\left\langle \frac{1}{2}\dot{\phi}^2 \right\rangle \sim \frac{A}{\tau^2}. \tag{5.49}$$

Now the potential is not quadratic, which means that kinetic and potential energy do not average at the same value. Virial theorem implies

$$\langle V(\phi) \rangle - V_- = 2\left\langle \frac{1}{2}\dot{\phi}^2 \right\rangle. \tag{5.50}$$

This means that the average value of the Lagrangian does not wash out, but asymptotically behaves as

$$-\langle \mathcal{L} \rangle \sim \frac{A}{\tau^2} + V_-. \tag{5.51}$$

If we calculate the stress-energy tensor

$$T^\mu{}_\nu = \dot{\phi}^2 \frac{x^\mu x_\nu}{-x_\lambda x^\lambda} - \mathcal{L}\delta^\mu{}_\nu, \tag{5.52}$$

it is now going to contain except for the kinetic energy of the wall, a cosmological constant like term that depends on the size of the bubble like

$$\Lambda \sim \frac{A}{\tau^2} + V_-, \tag{5.53}$$

where c depends on the specific parameters of our potential.

5.6 A candidate for dark energy

Let's now take a wild guess. Let's suppose that big bang was the emission of a bubble, so we are actually living inside a bubble with the size of the universe. Let's also suppose that the potential of the phase transition is well fit by the triangular approximation. It actually suffices that the potential in the region of the true vacuum is triangular. The natural selection of the potential parameters is that they are of Planck scale. Finally, let's suppose that the energy of the true vacuum is exactly zero.

Under these assumptions, we should today observe an effective cosmological constant of the order

$$\Lambda \sim \frac{M_{\text{Pl}}^2}{R_{\text{universe}}^2}, \tag{5.54}$$

which obviously depends on the age of the universe. The size of the observable universe today is about 10^{60} in Planck units. Thus, the cosmological constant we should observe in our scenario, would be

$$\Lambda \sim 10^{-120} M_{\text{Pl}}^4. \tag{5.55}$$

This is the right order of magnitude that we measure today [8–11].

With this model, we do not solve the original cosmological constant problem [12], namely why the vacuum energy of SM does not gravitate. Most probably we need more information on quantum gravity to resolve this. However, it resolves the cosmological constant problems that occurred after the recent measurement of it [13]. It explains its order of magnitude and if we assume that matter originates from the kinetic energy of bubble walls, then our model also explain why the matter content and dark energy content of our universe are of the same order of magnitude.

The idea of relating physical constants with cosmological quantities is not new at all. Paul Dirac in the 1930's observed that ratios of orders of magnitudes of cosmological quantities are similar to ratios of orders of magnitudes concerning the fundamental interactions. Conjecturing that this cannot be a coincidence, he expressed the large number hypothesis [14–16], according to which fundamental constants of nature, such as Newton's gravitational constant, depend on the age of the universe. The recent discovery of another large number, namely the ratio of the theoretical and observed vacuum energy densities, led to similar tries to connect the energy density of the vacuum with the age of the universe [17], as we do in this paper.

Additionally, the idea of the dark energy originating from a scalar is not new, too. Quintessence models can describe the dark energy content of the universe. In this approach, the dark energy is the effect of a slow rolling scalar field instead of one that performs a dumped oscillation, as in our case. The subject of quintessence is quite broad. A nice review is given in [18].

One critical objection about our model is the singular form of the potential at the position of the true vacuum. One should be able to find a model which predicts the existence of such a vacuum and moreover develop quantum field theory in the region of such a vacuum to show that the low energy effective description is also singular. However,

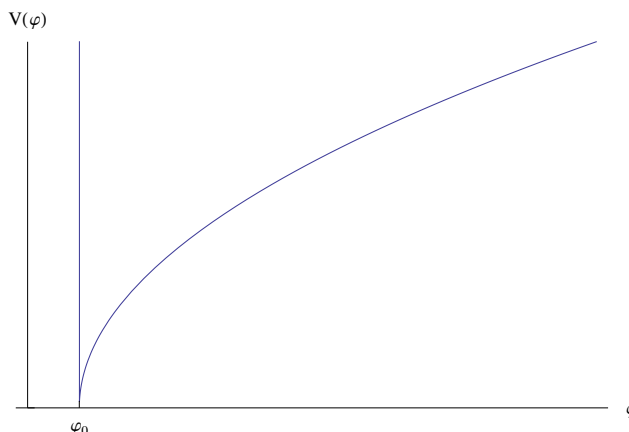


Figure 10. The form of the potential.

linear potential can occur by brane interactions in an orbifold like in the ekpyrotic scenario for the big bang [19–21]. Definitely further study is required on this field.

6 The asymptotic damped oscillation inside the bubble

6.1 The asymptotic solution for potential $V = a(\phi - \phi_0)^n$

It is interesting that the Stress-Energy tensor in the interior of the bubble has a direct dependency on the size of the bubble. It is also interesting that depending on the potential, this Stress-Energy tensor may represent a substance with negative pressure, thus providing a candidate for dark energy. Although it is impossible to find exact solutions for general form of the potential, we will try to calculate the asymptotic form of this damped oscillation for a potential of the form $V = a(\phi - \phi_0)^n$. In order to simplify things, we assume that the potential is infinite for $\phi < \phi_0$, or else ϕ_0 is the boundary of the configuration space. Thus, the solution gets reflected when it reaches ϕ_0 . This may represent an effective field theory, where the scalar is a moduli describing geometry of some brane configuration living in an orbifold.

We are interested in the damped oscillations a field performs around the area of the vacuum of a potential of the form

$$V(\phi) = \begin{cases} \infty, & \phi < \phi_0 \\ a(\phi - \phi_0)^n, & \phi > \phi_0. \end{cases} \quad (6.1)$$

The potential is sketched in figure 10.

Assuming a spherically symmetric solution, the equation of motion is

$$\ddot{\phi} + \frac{3}{\tau} \dot{\phi} = -V'(\phi), \quad (6.2)$$

where dot represents differentiation with respect to τ . If we define

$$\frac{1}{2} \dot{\phi}^2 + V(\phi) \equiv E, \quad (6.3)$$

the equation of motion can be written as

$$\dot{E} = -\frac{3}{\tau}\dot{\phi}^2. \tag{6.4}$$

This form of equation gives us a better point of view about how the system dissipates. We cannot find an exact solution to the above, but we expect that when τ is large, the losses are small in one period and thus, we can express the above equation as

$$\langle \dot{E} \rangle = -\frac{6}{\tau} \langle T \rangle, \tag{6.5}$$

where $T \equiv \frac{1}{2}\dot{\phi}^2$. Now we can use the explicit form for our potential

$$V = a(\phi - \phi_0)^n \tag{6.6}$$

and the virial theorem. The latter instructs us that

$$\langle T \rangle = \frac{n}{n+2} \langle E \rangle, \quad \langle V \rangle = \frac{2}{n+2} \langle E \rangle. \tag{6.7}$$

Using the above, equation (6.5) can be written

$$\langle \dot{E} \rangle = -\frac{6n}{n+2} \frac{\langle E \rangle}{\tau}, \tag{6.8}$$

whose solution trivially is

$$\langle E \rangle = c\tau^{-\frac{6n}{n+2}}. \tag{6.9}$$

The parameter c depends on the potential. If we assume that a characteristic mass scale of the potential is M_V , then the above solution behaves as

$$\langle E \rangle \sim \frac{M_V^{-2\frac{n-4}{n+2}}}{\tau^{\frac{6n}{n+2}}}. \tag{6.10}$$

If we are about to explain the dark energy content of the universe as this energy stored in the damped oscillation of the scalar field, we should check what is the appropriate value for the potential mass scale M_V . In such case, $\langle E \rangle$ has to equal the dark energy density measured today, and τ should equal the size of the observable universe R_U . Then, M_V must be

$$M_V \sim \langle E \rangle^{-\frac{1}{2}\frac{n+2}{n-4}} R_U^{\frac{3n}{n-4}}. \tag{6.11}$$

If we use $\langle E \rangle \equiv 10^{-120} M_p^4$ and $R_U = 10^{61} l_p$, we get the behaviour shown figure 11.

Here we would like to notice three interesting cases.

1. $n = 1$. This case has already been studied in section 5. The scale of the potential turns out to be the Planck scale, which obviously is a natural choice. Our result obviously agree with the results of the previous section.
2. $n = \frac{1}{2}$. In this case it turns out that $M_V = 10^{-17} M_p$, thus it is about 100 GeV, the electroweak scale. It could provide a connection to other known physics.
3. $n \rightarrow 0$. In this case the size of the universe does not help us at all to solve the hierarchy problem between the potential scale and the cosmological scale. We just convert the cosmological constant problem to a classical fine tuning problem, as we need a potential with characteristic scale the cosmological one.

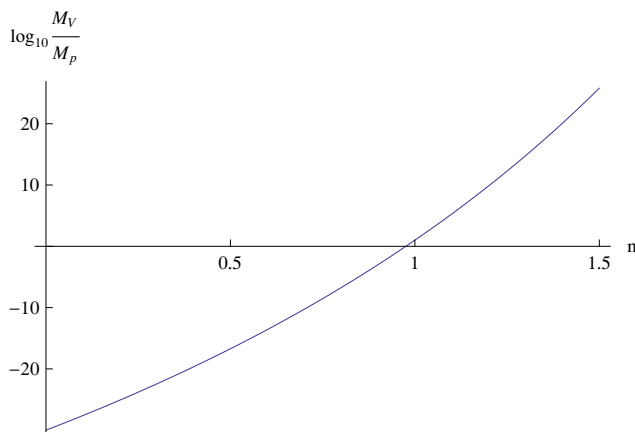


Figure 11. The scale of the potential as function of n .

6.2 The stress-energy tensor and the equation of state of the dark matter candidate

The stress-energy tensor is given by

$$T^\mu{}_\nu = \partial^\mu \phi \partial_\nu \phi - \mathcal{L} \delta^\mu{}_\nu. \quad (6.12)$$

Our solution depends only on proper time, thus

$$\partial_\nu \phi = \dot{\phi}(\tau) \frac{x_\nu}{\sqrt{x_\mu x^\mu}}. \quad (6.13)$$

Using the above, we get

$$T^\mu{}_\nu = \dot{\phi}^2 \frac{x^\mu x_\nu}{-x_\lambda x^\lambda} - \mathcal{L} \delta^\mu{}_\nu. \quad (6.14)$$

$$\langle T^\mu{}_\nu \rangle = 2 \frac{x^\mu x_\nu}{\tau^2} \langle T \rangle - \delta^\mu{}_\nu (\langle T \rangle - \langle V \rangle). \quad (6.15)$$

In the far future or in local coordinates, this is diagonal and describes an average energy density and pressure

$$\rho = \langle T \rangle + \langle V \rangle, \quad (6.16)$$

$$p = \langle T \rangle - \langle V \rangle. \quad (6.17)$$

Use of virial theorem is adequate to calculate

$$w \equiv \frac{p}{\rho} = \frac{n-2}{n+2}, \quad (6.18)$$

which is plotted in figure 12.

In the previous section we distinguished three interesting cases. It turns out that the calculated w for those is also interesting.

1. $n = 1$. In the case of a linear potential it turns out that $w = -\frac{1}{3}$. This is exactly the boundary case between an accelerating expanding universe and a decelerating one.

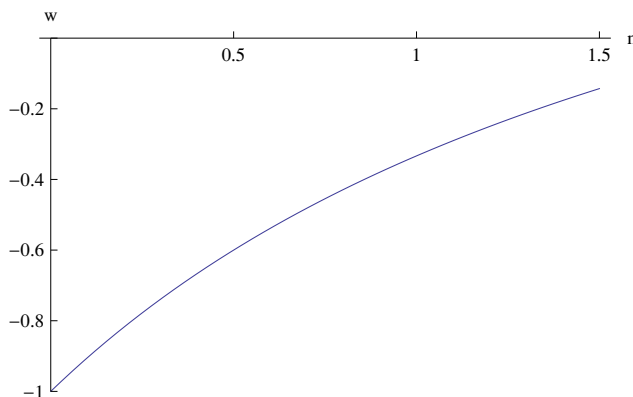


Figure 12. w as function of n .

2. $n = \frac{1}{2}$. In this case we find $w = -\frac{3}{5}$. This is not the most favoured value experimentally, however, it corresponds to an accelerating expanding universe.
3. $n \rightarrow 0$. This gives us $w = -1$ which is the most favourable value for the dark energy as measured today, and indistinguishable from a cosmological constant term, as long as the equation of state is considered.

We would like to notice here that although the equation of state does not agree for all selected cases with the measured one, there may be other resolutions to this problem. The stress energy tensor is made of two parts, one that obeys a matter equation of state corresponding to the kinetic energy of the wall and one, proportional to the Lagrangian density, that obeys the equation of state of a cosmological constant term. A possibility resolving the aforementioned problem is that the energy corresponding to the first term is wasted in particle creation leaving only the cosmological constant like term. More research is required in order to study this kind of scenarios.

6.3 Inhomogeneities in the dark content

We should not forget that actually the field performs an oscillation around the vacuum. That means that a fair question is whether the period of this oscillation is large enough in order to allow for measurable phenomena. If we neglect the dissipation term, we can estimate the period of the oscillation, just using conservation of E .

$$T = \sqrt{2} \int_{\phi_0}^{\phi_0 + \left(\frac{E}{a}\right)^{\frac{1}{n}}} \frac{1}{\sqrt{E - a(\phi - \phi_0)^n}} d\phi = \frac{\sqrt{2}\pi\Gamma\left(\frac{n+1}{n}\right)}{\Gamma\left(\frac{n+2}{2n}\right)} \frac{1}{\sqrt{E}} \left(\frac{E}{a}\right)^{\frac{1}{n}}. \quad (6.19)$$

As the period depends on E like $E^{\frac{1}{n} - \frac{1}{2}}$, for any n smaller than 2, it turns out that as universe grows, the period of the oscillations is getting smaller and smaller. If we use the experimental values for dark energy density and the radius of the universe, we result in a period of oscillations at our age, that is even smaller than the Planck time, thus making these oscillations experimentally unmeasurable.

Having such high frequency of oscillations seems peculiar, however, we study a strange field theory, where the potential around the vacuum is not harmonic. Further study on such field theories is required.

7 Discussion

We analysed tunneling solutions for some potentials that can provide us with analytic solutions. We learned several qualitative facts about phase transitions in field theory, as well as we acquired some useful tools.

The volcanic and ever better the smooth quadratic potential, can provide tools for calculating decay rates in several problems, where the thin wall approximation [1] does not apply. Of course, we already have the tools of rectangular and triangular approximation [3], however, as the decay rate per unit volume depends on the Euclidean action exponentially, a calculation of greater accuracy may be useful.

As the volcanic potential model teaches us, it is typical for such bubble solutions that the field never reaches the true vacuum in the interior of the bubble. Instead, it is performing a damped oscillation around it, whose amplitude is some kind of function of time that depends on the form of the potential around the true vacuum. This phenomenon may be of significant interest depending on the form of the potential.

The description of the barrier between the true and false vacuum by a non-convex potential generates questions about the uniqueness of the tunneling solution. Naively, such a potential corresponds to an oscillatory behaviour of the field at the region of the top of the barrier that could result in multiple solutions. Although we do not have a proof, the smooth quadratic potential example shows that this is not the case.

The smooth quadratic potential teaches us another interesting lesson. The size of the emitted bubble strongly depends on the curvature of the potential at the top of the barrier. In this toy example the size of the bubble is of the same order of magnitude of the inverse of the aforementioned curvature or at least the latter serves as a lower bound for the radius of the bubble. This has an interesting implication in the case of an asymptotically expanding universe. Typically, phase transitions in field theory occur at temperatures of the order of characteristic quantities of the potential describing the system. Masses are such quantities. Thus, according to our previous arguments, the size of emitted bubbles is going to be of the order of inverse temperature. Depending on the cosmological model, the radius of the universe is also a function of temperature, thus resulting in an upper bound for the possible number of bubbles emitted. This restricts the number of bubble collisions resulting in several cosmological predictions. Of course this is not going to be the case in a post-inflationary universe.

The most interesting result of our study is the fact that in a triangular potential, we observe an effective cosmological constant in the interior of the bubble that decreases as the bubble expands, in such a way that its scale asymptotically equals the geometric mean of the size of the bubble and the scale of the potential. Assuming that the parameters of the potential are of Planck scale and that the true vacuum energy vanishes, we make a very good prediction for the cosmological constant order of magnitude, which agrees with

what we measure today. Of course, this effective cosmological constant term is not the only contribution to the stress-energy tensor, resulting in the ratio of pressure to energy density in the interior of the bubble being larger than the experimentally favoured value -1 . However, the model we use contains only one scalar and is very simplistic. The idea may be useful in the construction of a more realistic model.

Later we extend our analysis to study the damped oscillation for a more general potential. It turns out that other interesting options also exist. If the potential is proportional to the square root of the field, then a potential with characteristic parameters of the electroweak scale predicts a dark energy content of the right order of magnitude and an accelerating universe.

Of course such a model for the cosmological constant predicts a vacuum energy that depends on the distance from the bubble wall, thus, on the position inside the bubble. Current experiments do not rule out such a dependence, thus, this is a direct experimental prediction of our model.

Such a time dependent cosmological constant is also predicted by quintessence models. The advantage of our approach is that the value of the observed cosmological constant is related with the size of the universe in a more direct way.

Moreover, even in the case of a quadratic potential there is still some non-trivial form for the stress-energy tensor that could have interesting cosmological implications in the expansion of the universe. In the case of more singular potentials, a connection with inflation could also be interesting. Finally, there is the open direction of generalizing to different potentials, or greater number of fields. Interesting behaviour, like the one we discovered in the triangular model, may appear in different cases. We believe that the most interesting future direction would be the inclusion of gravity into the problem. This way, we would be able to directly observe the effects of the discovered phenomena in the evolution of the universe.

Acknowledgments

I would like to especially thank D. Blas, L. Motl, K. Papadodimas and R. Rattazzi for useful discussions.

References

- [1] S.R. Coleman, *Fate of the false vacuum. 1. Semiclassical theory*, *Phys. Rev. D* **15** (1977) 2929 [Erratum *ibid.* **D 16** (1977) 1248] [[INSPIRE](#)].
- [2] C.G. Callan Jr. and S.R. Coleman, *Fate of the false vacuum. 2. First quantum corrections*, *Phys. Rev. D* **16** (1977) 1762 [[INSPIRE](#)].
- [3] M.J. Duncan and L.G. Jensen, *Exact tunneling solutions in scalar field theory*, *Phys. Lett. B* **291** (1992) 109 [[INSPIRE](#)].
- [4] T. Hamazaki, M. Sasaki, T. Tanaka and K. Yamamoto, *Self-excitation of the tunneling scalar field in false vacuum decay*, *Phys. Rev. D* **53** (1996) 2045 [[gr-qc/9507006](#)] [[INSPIRE](#)].

- [5] K. Koyama, K. Maeda and J. Soda, *An open universe from valley bounce*, *Nucl. Phys. B* **580** (2000) 409 [[hep-ph/9910556](#)] [[INSPIRE](#)].
- [6] S.R. Coleman, *Spherical symmetry of action minima for Euclidean scalar fields*, HUTP-77-A020, Harvard University, Cambridge U.S.A. (1977) [[INSPIRE](#)].
- [7] K.-M. Lee and E.J. Weinberg, *Tunneling without barriers*, *Nucl. Phys. B* **267** (1986) 181 [[INSPIRE](#)].
- [8] SUPERNOVA SEARCH TEAM collaboration, A.G. Riess et al., *Observational evidence from supernovae for an accelerating universe and a cosmological constant*, *Astron. J.* **116** (1998) 1009 [[astro-ph/9805201](#)] [[INSPIRE](#)].
- [9] SUPERNOVA COSMOLOGY PROJECT collaboration, S. Perlmutter et al., *Measurements of Ω and Λ from 42 high redshift supernovae*, *Astrophys. J.* **517** (1999) 565 [[astro-ph/9812133](#)] [[INSPIRE](#)].
- [10] J.C. Baker et al., *Detection of cosmic microwave background structure in a second field with the cosmic anisotropy telescope*, *Mon. Not. Roy. Astron. Soc.* **308** (1999) 1173 [[astro-ph/9904415](#)] [[INSPIRE](#)].
- [11] SDSS collaboration, M. Tegmark et al., *Cosmological parameters from SDSS and WMAP*, *Phys. Rev. D* **69** (2004) 103501 [[astro-ph/0310723](#)] [[INSPIRE](#)].
- [12] S. Weinberg, *The cosmological constant problem*, *Rev. Mod. Phys.* **61** (1989) 1 [[INSPIRE](#)].
- [13] S. Weinberg, *The cosmological constant problems*, [astro-ph/0005265](#) [[INSPIRE](#)].
- [14] P.A.M. Dirac, *The cosmological constants*, *Nature* **139** (1937) 323 [[INSPIRE](#)].
- [15] P.A.M. Dirac, *New basis for cosmology*, *Proc. Roy. Soc. Lond. A* **165** (1938) 199 [[INSPIRE](#)].
- [16] S. Ray, U. Mukhopadhyay and P. Pratim Ghosh, *Large number hypothesis: a review*, [arXiv:0705.1836](#) [[INSPIRE](#)].
- [17] L. Nottale, *Mach's principle, Dirac's large numbers and the cosmological constant problem* (1993).
- [18] E.J. Copeland, *Dynamics of dark energy*, *AIP Conf. Proc.* **957** (2007) 21 [[INSPIRE](#)].
- [19] G.W. Moore, G. Peradze and N. Saulina, *Instabilities in heterotic M-theory induced by open membrane instantons*, *Nucl. Phys. B* **607** (2001) 117 [[hep-th/0012104](#)] [[INSPIRE](#)].
- [20] J. Khoury, B.A. Ovrut, P.J. Steinhardt and N. Turok, *The ekpyrotic universe: colliding branes and the origin of the hot big bang*, *Phys. Rev. D* **64** (2001) 123522 [[hep-th/0103239](#)] [[INSPIRE](#)].
- [21] R. Brandenberger and F. Finelli, *On the spectrum of fluctuations in an effective field theory of the ekpyrotic universe*, *JHEP* **11** (2001) 056 [[hep-th/0109004](#)] [[INSPIRE](#)].